Spectroscopic Analysis of Chain Conformation Distribution in a Biodegradable Polyester Elastomer, Poly(β-hydroxyoctanoate)

Hun-Jan Tao, William J. MacKnight, K. D. Gagnon, R. W. Lenz, and Shaw L. Hsu*

Polymer Science and Engineering Department and Materials Research Science and Engineering Center, University of Massachusetts, Amherst, Massachusetts 01003

Received May 5, 1994; Revised Manuscript Received December 8, 1994®

ABSTRACT: Chain conformational distribution of a biodegradable polyester elastomer, poly(β-hydroxyoctanoate) (PHO), has been analyzed using vibrational spectroscopy in conjunction with normal vibrational analysis. For the as-prepared, mainly amorphous materials, side-chain conformation distribution is extremely broad and is consistent with the expected three-state rotational isomeric model. On the basis of our vibrational analysis, we have established that side-chain conformational distribution transforms to one containing mainly the extended form after thermal annealing. In contrast, the conformational distribution of the side chains remains unchanged as a function of strain. Additionally, the carbonyl stretching vibrations were found to be sensitive to changes in the crystalline environment and thus can be utilized to monitor the degree of crystallinity in these samples. Even though the exact mechanism has not been identified, these results indicate that changes in crystallinity or side-chain conformational distribution cannot be responsible for the extremely high tensile set observed.

Introduction

Poly(β-hydroxyoctanoate) (PHO) is a polyester produced by bacteria *Pseudomonas oleovorans* which grow on sodium octanoate or octane as the carbon source under a limited nutrient or a lack of oxygen condition.[1-3] This polymer, considered as an energy storage material, accumulates as intracellular granules in response to this sort of environmental stress. This sensitivity also makes them inherently biodegradable. The resultant polyester is a random copolymer rather than a homopolymer because the metabolism of the bacteria can either add or cleave off two carbons from the food source molecules. The structure and composition of PHO are shown in Figure 1. This polymer is isotactic due to the absolute [R] configuration of the chiral carbons making them to be crystallizable. However, the degree of crystallinity is only approximately 30% due to the random copolymer nature.[4] These crystalline domains act as physical cross-links for the rest of non-crystalline, low-T_g (−35 °C) chains resulting in its thermoplastic elastomer feature.

PHO will crystallize as a 2_1 helix in an orthorhombic lattice with two molecules per unit cell.[4] The side chains were proposed to form ordered sheets with extended conformation in the crystalline structure.[4] The fiber repeat is 4.55 Å, which is smaller than poly(β-hydroxybutyrate) (PHB), 5.96 Å, and poly(β-hydroxyvalerate) (PHV), 5.56 Å. This collapse in the *c* dimension has been postulated to be driven by changes in side-chain packing.[4] The crystallization rate of PHO is extremely slow.[1-5] The low degree of crystallinity and the slow crystallization rate are directly attributable to the random nature of the main-chain sequence as well as the long side chains.

PHO possesses very high permanent tensile sets under deformation.[1,2] For example, the tensile sets are 40%, 80%, and 230% for PHO under strains of 100%, 150%, and 300%, respectively.[1,2] This behavior limits its applicability as a practical thermoplastic elastomer.

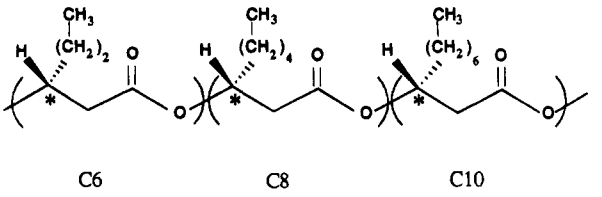

Composition	Description of Repeat Units
10%	C6 = β-hydroxyhexanoate
86%	C8 = β-hydroxyoctanoate
4%	C10 = β-hydroxydecanoate

Figure 1. Chemical structure of bacterially produced poly(β-hydroxyoctanoate) (PHO) random copolyester. Carbons with asterisks are the chiral centers.

The permanent tensile sets have been attributed either to a change in sample crystallinity or to strain-induced side-chain crystallization.[1,2] However, without a convincing way to characterize the chain conformational change, it is difficult to confirm these conjectures.

In this study, we utilized Fourier transform Raman spectroscopy as the principal tool to analyze chain conformation. It is expected that the Raman spectra obtained for PHO are characteristic of the chain conformation because many of the bands are expected to be associated with the large polarizability changes of the C−C bonds along either the main or side chains. Because quantitative structural information is needed, we have also carried out normal vibrational analyses in conjunction with our experimental result. Generally speaking, a detailed normal vibrational analysis can describe the nature of the normal vibrations, their frequencies, and densities of state. Computer programs used for such studies are really capable of calculating only one specific chain conformation. In this study, we have adopted the computer programs developed by Snyder and his co-workers which would yield both frequency and band intensity for an assembly of disordered chains.[6,7] The dihedral angles along the chain for each conformation are generated according to the statistical weights calculated using the relative energy

* To whom correspondence should be addressed.
® Abstract published in *Advance ACS Abstracts,* February 15, 1995.

0024-9297/95/2228-2016$09.00/0

of an individual rotational isomeric state. The composite spectrum obtained makes it possible to investigate the conformational distribution change of PHO side chains during the crystallization and when being deformed. Our results are reported here.

Experimental Section

The biosynthetic procedure of PHO and its characterization have been described previously.[1-5,8,9] For deformation experiments, PHO which crystallized at 5 °C for 36 days was cut to 2 cm by 2 mm stripes with a thickness of 1 mm. The sample was stretched with a stretcher and kept for 10 min at several elongation ratios. After releasing the stress, the permanent tensile set was recorded.

Raman spectra were obtained on a Bruker 88 Fourier transform Raman bench with laser excitation provided by a Nd:YAG laser (1064 nm) in the near-infrared region. Incident laser power was maintained at 300 mW. Typically, 2000 scans were coadded to achieve an acceptable signal-to-noise ratio. All the spectra were obtained with a backscattering geometry. Spectral resolution was maintained at 4 cm^{-1}. Curve deconvolution was carried out with the software LAB CALC (Galactic Ind. Corp.). For the long-term phase transformation study, PHO was loaded into the sample die and was heated at 100 °C under vacuum for 2 h. After cooling to room temperature, the Raman spectrum was taken and was named as "Day 1". Generally, each spectroscopic measurement takes 2 h. There is no evidence that the samples changed after being irradiated by the laser beam. After recording each spectrum, each individual sample was sealed in a bottle with anhydrous calcium sulfate to keep it dry. Then the sample was kept under 5 °C until the next experiment.

Optical circular dichroism (CD) was performed on AVIV 62DS (AVIV Associates, Inc.) equipped with a xenon arc lamp and MgF_2 linear polarizer. A photoelastic modulator (PEM) was operated at 50 kHz. Spectra were taken for the 175–400 nm region. PHO samples were casted on the external surface of a 1-mm-thick quartz cell from a 2% chloroform solution. The solution was filtered with a 0.2-μm disposable syringe filter. The casted sample film was heated at 100 °C for 2 h before the first spectrum was recorded. For long-term studies, the sample storage procedure was the same as that used in the Raman study. For each scan the spectral resolution was maintained at 0.5 nm.

Computational Methods

Normal-coordinate calculation for the isotropic Raman spectrum of an assembly of disordered chains was performed with a program written by Snyder and his co-workers.[6,7] The procedure has been published earlier and is briefly summarized as follows. The intensity of the Raman spectrum, $I(\nu)$, is determined by scattering activity, $S(\nu)$, and a Boltzmann factor, $B(\nu)$, shown below

$$I(\nu) = S(\nu)/B(\nu) \tag{1}$$

$$B(\nu) = \nu[1 - \exp(-h\nu/kT)] \tag{2}$$

where ν, h, k, and T are the vibrational frequency, Planck's constant, Boltzmann's constant, and absolute temperature, respectively. The scattering activity for the Raman spectrum of an assembly of disordered chains was approximated by

$$S(\nu) = \sum_{M=1}^{M_T} S^M(\nu) \tag{3}$$

where $S^M(\nu)$ is the scattering activity of random conformer M generated by the Monte Carlo method, and M_T is the number of conformers in the ensemble. $S^M(\nu)$ is calculated by the bond polarizability model[7] according to the following expression

$$S_k \propto [\sum_i L_{ik}^R + D\sum_j L_{jk}^\omega]^2 \tag{4}$$

where S_k is the scattering activity of normal mode k, L_{ik}^R is the normal-coordinate element for the ith CC stretching (R) internal coordinate, and L_{jk}^ω is that for the jth CCC bending (ω) coordinate. D in eq 4 is the intensity parameter which is defined as the ratio of mean polarizability derivatives for CCC bending to CC stretching. The intensity parameters for all the backbone CC bonds and CCC angle bendings are assumed to be identical and have been taken to be conformally invariant. The intensity contributions from CH stretching and CC torsion are ignored because we are principally interested in the skeletal modes in the 700–1000 cm^{-1} region.[6,7] Snyder's method has been demonstrated previously to successfully reproduce the vibrational spectra of several n-alkanes.[6,7] As an example, the calculated isotropic Raman spectrum of n-hexane and the experimental data are shown in Figure 2. Both frequencies and relative intensity of these skeletal vibrations have been reproduced well. All the parameters used in this example have been published previously.[6,7]

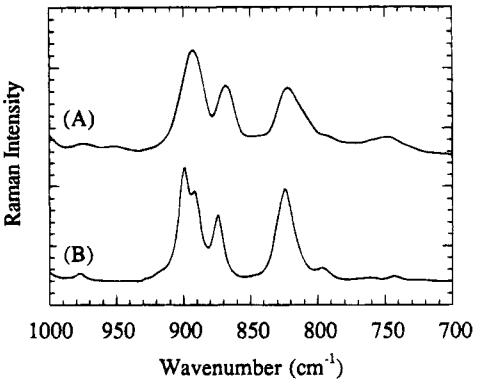

Figure 2. Raman spectra of n-hexane: (A) measured Fourier transform Raman spectrum and (B) calculated spectrum with an energy difference of 800 cal/mol between trans and gauche states. A total of 500 conformers was generated for this calculation.

Our objective is to calculate Raman-active skeletal vibrations assignable to PHO side chains in order to characterize their conformations. We used the model structure shown in Figure 3 as an approximation for PHO side chains. The perturbative effects associated with coupling to the main chain are implicitly incorporated in the effective masses used for the atoms which are attached to the main chain (atoms 2 and 3 in Figure 3). The force constants for the model structure are assumed to be unaffected. Therefore, force constants for aliphatic ether compounds have been used in our analysis.[10] The choice of the effective mass for atoms 2 and 3 is somewhat arbitrarily. In our analysis, the effective mass of atom 2 (20 amu) was taken to be [(atom 2 + atom 6 + atom 7) + (atom 5)/2]. The effective mass for atom 3 (22 amu) was taken as [atom 3 + (atom 4)/2]. Different values chosen for the effective mass of atoms 2 and 3 will shift the calculated frequency and intensity in the skeletal modes somewhat but not significantly.

We are interested in the composite spectrum for an ensemble of chains with different chain conformations.

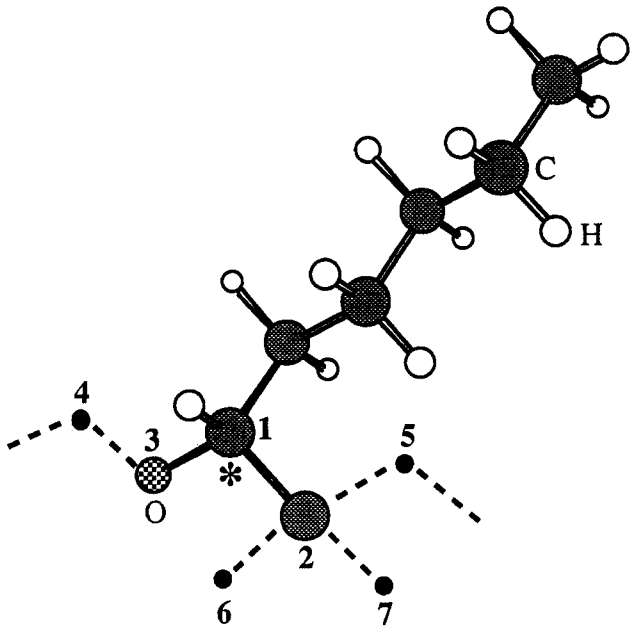

Figure 3. Stereochemical representation of the model structure of a PHO side chain used in the normal-coordinate analysis. Dashed lines and solid spots are used to illustrate the main-chain position and are not included in the model structure. The carbons with the asterisk is the chiral center.

We have utilized Flory's rotational-isomeric-state (RIS) model, with one trans and two gauche states.[11] A total of 2000 conformers was generated for vibrational analysis. The relative population for each conformation is determined by the following condition:

$$W^M = n_s{}^M \exp(-E^M/RT) \tag{5}$$

where W^M is the weight for a particular conformer, $n_s{}^M$ is its statistical weight, and E^M is its energy with the all-trans conformation as the zero point. Its value is calculated by

$$E^M = n_G E_G + n_{GG}{}^* E_{GG}{}^* \tag{6}$$

In eq 6, n_G is the total number of gauche bonds and $n_{GG}{}^*$ is the number of GG* pairs. E_G and $E_{GG}{}^*$ are the corresponding energies.[11] The pentane effect for the steric hindrance of the GG* conformation has been taken into consideration.[11] The dihedral angles for the trans and gauche states were taken to be 180° and 67°, respectively. A variation of 10° was used to allow some fluctuations about the local energy minima to incorporate the internal-rotation broadening effect.[6] For each conformer, the dihedral angles were assigned by the Monte Carlo method based on the probability of the RIS model.[6,7] The population distribution for T, G, and G* can be adjusted by changing the energy differences.

Force constants were automatically picked up in a force constant library by checking the atomic type of each atom and its local geometry for each conformer. To calculate relative band intensity, specific parameters related to polarizability changes were adopted form previous studies of *n*-alkanes.[6,7] We have assumed that the ester unit on the backbone will not change the polarizability derivatives of the aliphatic side chains significantly. The spectra were constructed by the histograms of scattering power at the frequency region of interest with an internal of 2 cm^{-1}. A Lorentzian line shape with a bandwidth (fwhm, full width at half-maximum) of 8 cm^{-1} was used for each peak in the histogram. Then spectra including temperature effect were calculated using eq 2.

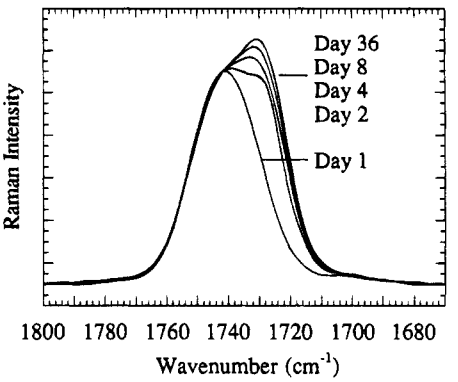

Figure 4. Variation of the carbonyl stretching region for the PHO crystallization process measured by Fourier transform Raman spectroscopy. Time increases from bottom to top. All of the spectra were normalized with respect to the 1742 cm^{-1} intensity.

Finally, molecular simulation was utilized to calculate the contour energy map of a PHO chain repeat using POLYGRAF (Molecular Simulations, Inc.). A Dreiding II force field[12] was used, and the electrostatic charges were calculated by the Gasteiger method.[13] Each dihedral angle was varied from 0° to 360° with a 6° increment. A conjugate-gradient method was employed for minimizing energy. Typically, the incremental decrease of the overall energy term per step is less than 0.1 (kcal/mol)/Å within 300 steps.

Results and Discussion

1. Characterization of Chain Conformation. The principal objective of this study is to evaluate the structural changes of these biodegradable polyesters induced by thermal annealing and during mechanical deformation. The carbonyl stretching region was found to be an appropriate region to monitor the PHO main-chain conformational change. Figure 4 is the FT-Raman spectra of PHO during the thermal annealing process in the carbonyl stretching region. There are two distinct bands located at 1742 and 1731 cm^{-1}. These two components cannot be assigned to crystal field splitting since strong specific intermolecular interactions do not exist. Infrared spectroscopy shows that only negligible amounts of residual hydroxy groups in PHO were found. Therefore, this splitting is not caused by hydrogen bonding. In a previous Raman study on other ester compounds, a similar doublet has been observed and was assigned to different carbonyl groups dispersed in amorphous and crystalline phases.[14,15] The lower frequency band is assigned to the crystalline state, while the higher one is for the amorphous phase.[14,15] The PHO main chain has a 2_1 helical conformation in the crystalline state.[4] Therefore, we have assigned the 1742 and 1731 cm^{-1} components to be associated with carbonyl groups for disordered and helical chains, respectively. The relative intensity of these two bands can be used to monitor the change in crystallinity even though their absolute amounts are difficult to evaluate.

Figure 4 clearly shows that, even though most of the crystallization occurs within 1 week, the process continues for a long period of time at a lower rate. Furthermore, another conformation-sensitive region in 1200–700 cm^{-1} is depicted in Figure 5. From changes in 870 and 1100 cm^{-1} bands in Figure 5, it also can be shown that the chain conformation keeps changing even

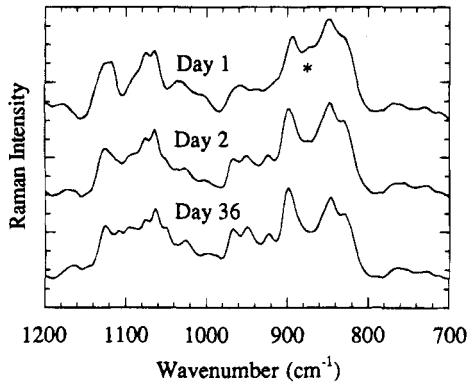

Figure 5. Variation of Fourier transform Raman spectra in the region of 700−1200 cm^{-1} for the PHO phase transformation process. The position with the asterisk is the one of the side-chain skeletal mode band which is sensitive to its conformation.

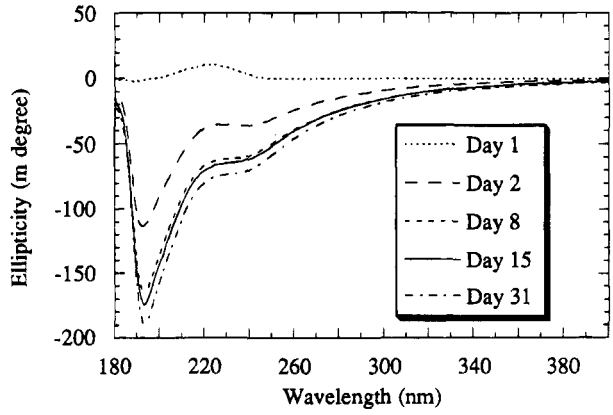

Figure 6. Variation of optical circular dichroism for the PHO phase transformation process. Time increases from top to bottom.

after 36 days. The observed slow crystallization process is consistent with the previous DSC study.[1,2,14,15] These data are inconsistent with previous WAXS and solid NMR studies which indicated that the crystallization process could be completed within a period as short as 6 h.[4] The discrepancy may be attributed to the sensitivity limitation of these methods. To assure that the changes in the carbonyl stretching region can really be correlated to changes in the main-chain conformation, we have also conducted circular dichroism studies.

Circular dichroism (CD) absorption can occur from an asymmetric secondary structure and is known as an extremely sensitive tool to monitor the chain conformation change.[16] The optical activity studies of PHB and similar compounds were well documented, and those results would be used to assign the bands observed for PHO.[17-20] For amorphous PHO, there is a weak CD band located at 220 nm which is due to the Cotton effect of an ester n $\rightarrow \pi^*$ transition. This feature is shown in Figure 6 for the Day 1 curve. The strong ester $\pi \rightarrow \pi^*$ transition occurs at a wavelength which is lower than the instrument detection limit so it cannot be observed for amorphous PHO. On the other hand, when PHO crystallizes, some of its ester main chains change their conformations to the left-handed 2_1 helix. This asymmetric helical structure structure will split the ester $\pi \rightarrow \pi^*$ transition into two peaks with opposite signs.[16,21] The CD spectrum for semicrystalline PHO clearly shows this splitting (only half of the splitting was detected due to the detection limit). The intensity of this band can be correlated to the degree of phase transformation. Figure 6 shows that the crystallization process lasts for a very long time even though most of the crystallization does occur in the first week. This result is consistent with our Raman finding described above and previous DSC observations.[1,2] Thus the relative intensities of carbonyl stretchings are directly related to the different main-chain conformations and can be used to monitor the crystallization process.

The preferred 2_1 helix associated with the main-chain conformation of PHO is well established. In contrast, the conformation distribution of side chains is far from clear. A previous solid-state NMR study revealed that the conformation of PHO side chains can be different depending on the degree of crystallinity of the sample.[4] Wide-angle X-ray diffraction results have suggested that side chains may form ordered sheets with extended structure in crystalline regions.[3,4] Nevertheless, a convincing structural assignment regarding PHO side chains was never achieved. Raman spectroscopy is particularly suitable for studying chain conformations, especially using the skeletal vibrations (CC stretching or CCC angle bending vibrations) in the 800−1000 cm^{-1} region. Characteristic bands for ester groups on the main chain are expected to be located at 850 and 960 cm^{-1}. Based on the methyl propionate study, these bands are assignable to ester CC stretching and CO stretching, respectively.[14] As can be seen from the Raman spectra shown in Figure 5, the 870−900 cm^{-1} region is a suitable region for monitoring side-chain conformation without complications from Raman-active vibrations associated with the main chain.

The two bands in the region of 870−900 cm^{-1} (Figure 5) are obtained from the original measured spectrum using a curve-fitting technique (A-2 and B-2 in Figure 7). To characterize this region, we conducted a normal-coordinate calculation for the PHO side chain. We have generated two types of side chains. First, using the rotational-isomeric-state model, we generated 2000 random conformers based on the statistical weight for each individual state. In addition, the program allows the possibility to calculate a chain of specific chain conformation, in this case, one with a planar zigzag fully extended structure. The population statistics of the generated 2000 random conformers are adjusted to match the experimental result (Figure 7A-2). The composite spectrum with overall 80.93% trans structures turns out to be very close to the experimental observation (Figure 8A). A detailed population statistics is listed in the inset of Figure 8A. Furthermore, the calculated Raman spectrum for a fully-extended side chain is shown in Figure 8B. From this calculation it clearly shows that bands at 895 and 880 cm^{-1} correspond to an extended side chain and less extended structures, respectively. Comparing Figures 7 and 8 we conclude that the PHO side chains possess a more extended structure for crystalline PHO than for amorphous PHO. This result is consistent with the previous solid-state NMR observation that PHO side chains have different conformations in the amorphous state and in the crystalline state.[4] It also confirms the conjecture by WAXS study that PHO side chains are likely to form a sheetlike structure with an extended conformation in the crystalline state.[4] Thus, by monitoring the change in the 870−900 cm^{-1} region for deformed samples, we can understand whether there is any strain-induced crystallization in the PHO side chains.

2. Molecular Mechanism of Deformation. Three mechanisms for the permanent tensile set of PHO have

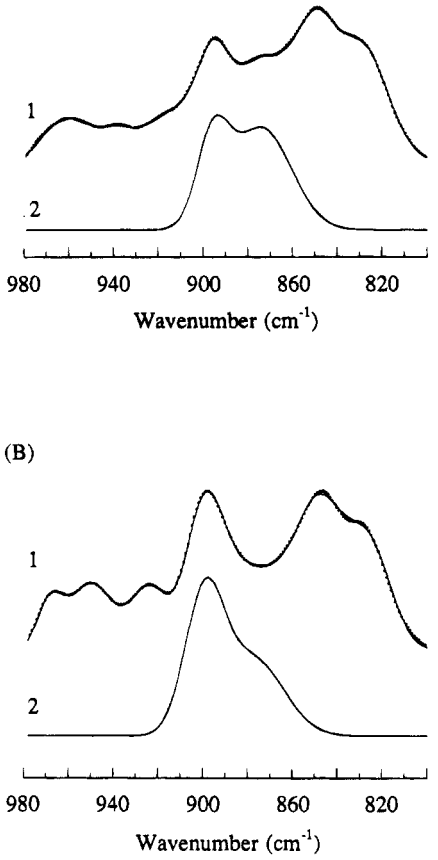

Figure 7. Measured Raman spectra for PHO at different levels of phase transformation: (A) amorphous state and (B) semicrystallinity state. (1) Dots are experimental data, while the solid line is the curve-fitting result. (2) The deconvoluted bands are associated with the side-chain skeletal mode.

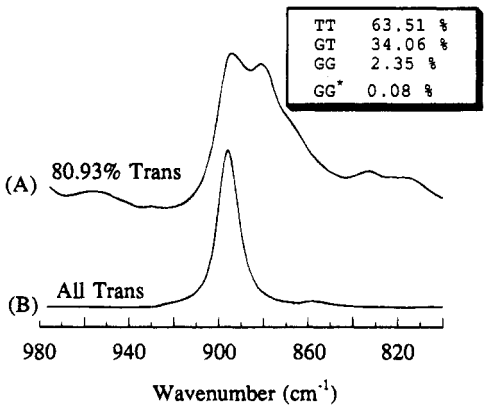

Figure 8. Calculated Raman spectra for the PHO side-chain model structure as shown in Figure 3: (A) for a non-fully-extended structure with the dihedral angle statistics shown in the inset; (B) for a fully-extended side chain.

been proposed previously:[1,2] (1) permanent orientation or displacement (flow) of the physical crosslinks in the amorphous matrix; (2) irreversible strain-induced crystallization; (3) deformation-induced breakup or rearrangement of the physical crosslinks. The second and third hypotheses can be analyzed using carbonyl stretchings and side-chain skeletal vibrations. For deformed PHO's with various levels of permanent tensile sets, changes in the carbonyl region are shown in Figure 9. The degree of crystallinity dropped slightly for samples stretched up to 150% strain (tensile set 85%) (Figure 9A). At even higher elongations there indeed is a slight increase in crystallinity (Figure 9B). We have no

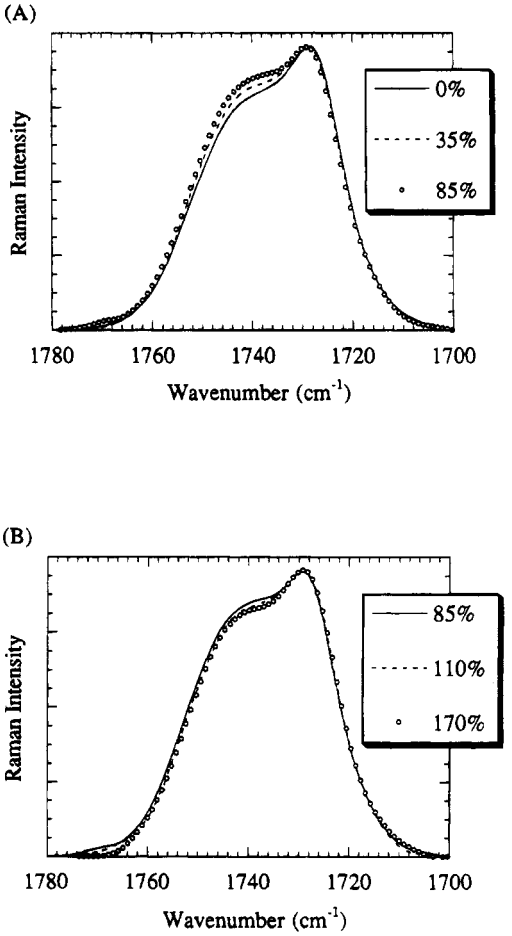

Figure 9. Variation of the carbonyl stretching region of stretched PHO's measured by Fourier transform Raman spectroscopy. The inset indicates the values of permanent tensile sets for PHO samples after various levels of mechanical elongation.

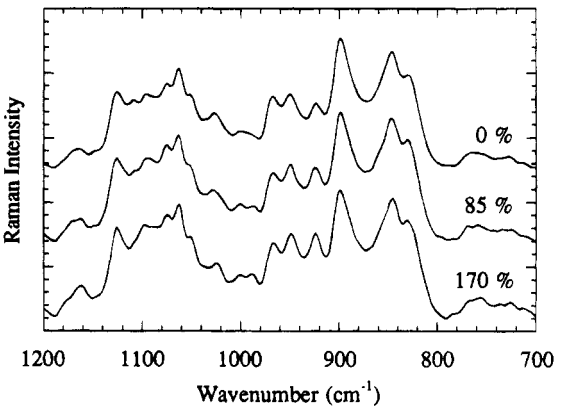

Figure 10. Variation of Fourier transform Raman spectra in the region of 700–1200 cm^{-1} for deformed PHO samples. Listed values are the permanent tensile sets.

evidence, however, to show any significant strain-induced change in the main-chain conformation or, indirectly, changes in the degree of crystallinity for deformed PHO's. By examining the side-chain skeletal vibrations in the 870–900 cm^{-1} region (Figure 10), there is also no evidence to show any significant strain-inducing ordering for PHO side chains. Furthermore, our WAXS study indicated that for a deformed PHO sample with a 170% tensile set the change in the crystal size is negligible. It should be pointed out, however, that previous DSC studies for deformed PHO's have suggested an increase in the heat of fusion and a

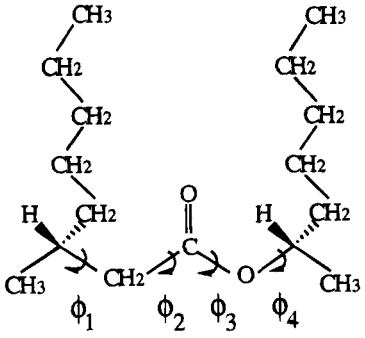

Figure 11. Model structure of PHO used for calculating the contour maps of conformational energy. ϕ_1–ϕ_4 are the dihedral angles in the backbone. The dihedral angle is taken to be 180° for the trans conformation.

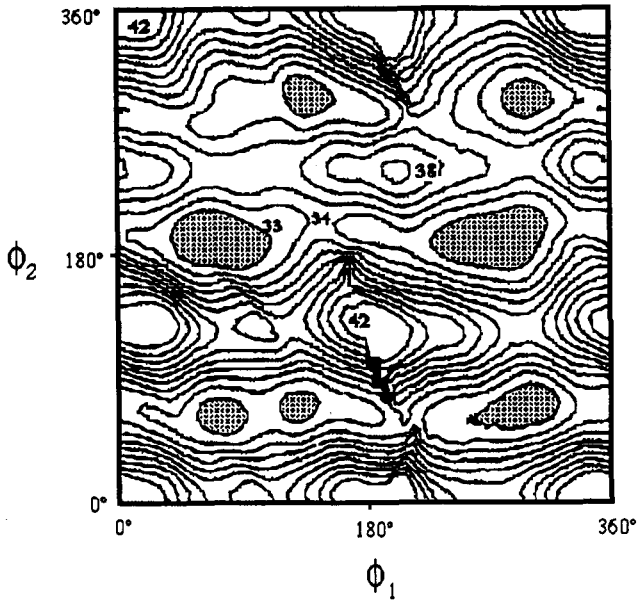

Figure 12. Contour map of conformational energy for the model structure shown in Figure 10. Listed values are the potential energies in kcal/mol. The increment for each interval is 1 kcal/mol.

decrease in the melting point as a function of strain.[1,2] We have no explanation for those observations.

When deformed, polarized optical microscopy reveals a considerable amount of anisotropy.[4] WAXS study also showed that the chain axis of the crystals will tend to orient parallel to the stretching direction.[4] With these findings, we suspect that the permanent tensile set results from the irreversible change in chain orientation coupled with changes in the chain conformation, but not necessarily crystallinity. We suggest that mechanical elongation induces more extended chains. After releasing from the stress, thermal energy is not sufficiently high to overcome the energy barrier between gauche/trans states; thus, the amorphous chains are trapped by the more extended conformation. This conjecture can be supported by our molecular simulation study. In that calculation, we used the PHO structure shown in Figure 11. There are four dihedral angles for each repeat unit. However, because each repeat unit has similar structures for both sides with respect to the carbonyl group (Figure 11), we can, similar to the approximation used previously, sequentially change ϕ_1 and ϕ_2 but let rest of the chain relax.[22,23] The calculated contour map is shown in Figure 12. The locations of energy minima are exhibited as gray areas. The global minimum is along the line of $\phi_2 = 180°$, while other local minima

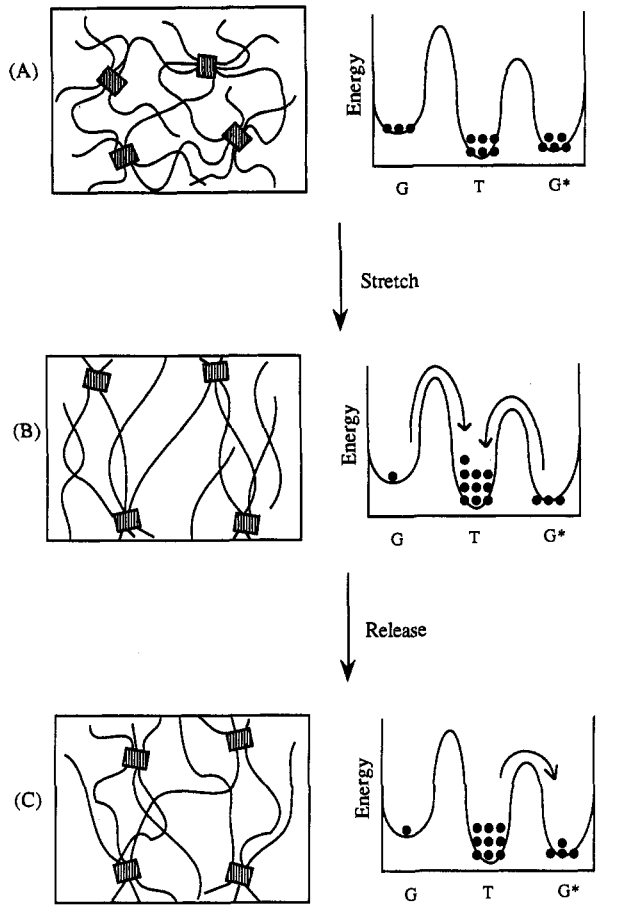

Figure 13. Schematic representation of the proposed mechanism for the PHO permanent tensile set: (A) undeformed state; (B) sample under elongation; (C) sample after releasing from the elongation. The molecular model for the chain conformation is shown in the left column with its corresponding conformation distribution in the right column. The number of dots is a representation for the population. T stands for trans conformation. G and G* stand for gauche conformations. A change in the population in B is caused by mechanical deformation. A change in the population in C is caused by the thermal energy.

occur at the gauche ϕ_2 conformations. The energy barrier between trans and gauche states is very high (≈10 kcal/mol) due to steric interactions with side chains. This result is consistent with our hypothesis. Our proposed model for the permanent tensile set of a PHO elastomer is summarized by the schematic representation shown in Figure 13. The high rotational energy barrier between different conformations for the amorphous chains resulting from the long side chains is responsible for this tensile set.

Conclusions

Fourier transform Raman spectroscopy in conjunction with normal-coordinate analysis have provided spectroscopic features useful for conformational analysis. The increase in sample crystallinity can be directly correlated to an increase in the helical conformation. It is also shown that the long side chain of PHO will take a more extended structure in the crystalline state compared with the amorphous state. The carbonyl stretching region can be used to monitor the change in crystallinity during the phase transformation and mechanical deformation processes. It is found that the crystallization process is extremely slow. It is also found that mechanical deformation has no significant effect

on the crystallinity. The breakup of crystalline domains and the strain-induced crystallization are believed not to be the important reasons for the high permanent tensile set associated with PHO. The irreversible orientation and displacement of amorphous chains due to the steric interaction between long side chains is believed to be the dominating factor for this feature.

Acknowledgment. This research has been supported by a grant from the Army Research Office, Grant No. DAAL03-91-G-0127, and funding from the NSF Materials Research Science and Engineering Center.

References and Notes

(1) Gagnon, K. D.; Lenz, R. W.; Farris, R. J.; Fuller, R. C. *Rubber Chem. Technol.* **1992**, *65*, 761.
(2) Gagnon, K. D.; Lenz, R. W.; Farris, R. J.; Fuller, R. C. *Macromolecules* **1992**, *25*, 3723.
(3) Gross, R. A.; DeMello, C.; Lenz, R. W.; Brandl, H.; Fuller, R. C. *Macromolecules* **1989**, *22*, 1106.
(4) Marchessault, R. H.; Monasterios, C. J.; Morin, F. G.; Sundararajan, P. R. *Int. J. Biol. Macromol.* **1990**, *12*, 158.
(5) Richtering, H. W.; Gagnon, K. D.; Lenz, R. W.; Fuller, R. C.; Winter, H. H. *Macromolecules* **1992**, *25*, 2429.
(6) Snyder, R. G. *J. Chem. Soc., Faraday Trans.* **1992**, *88*, 1823.
(7) Snyder, R. G.; Kim, Y. *J. Phys. Chem.* **1991**, *95*, 602.
(8) Brandl, H.; Gross, R. A.; Lenz, R. W.; Fuller, R. C. *Appl. Environ. Microbiol.* **1988**, *54*, 1977.
(9) Gagnon, K. D.; Bain, D. B.; Lenz, R. W.; Fuller, R. C. In *Novel Biodegradable Microbial Polymers*; Dawes, E. A., Ed.; Kluwer Academic Publishers: Dordrecht, The Netherlands, 1990; pp 449 and 450.
(10) Snyder, R. G.; Zerbi, G. *Spectrochim. Acta* **1967**, *23A*, 391.
(11) Flory, P. J. *Statistical Mechanics of Chain Molecules*; Hanser Publishers: New York, 1989.
(12) Mayo, S. L.; Olafson, B. D.; Goddard, W. A., III *J. Phys. Chem.* **1990**, *94*, 8897.
(13) Gasteiger, J. *Tetrahedron* **1980**, *36*, 3219.
(14) Moravie, R. M.; Corset, J. *J. Mol. Struct.* **1975**, *24*, 91.
(15) Mido, Y.; Shono, T. *J. Mol. Struct.* **1991**, *246*, 13.
(16) Charney, E. *The Molecular Basis of Optical Activity*; John Wiley & Sons: New York, 1979.
(17) Marchessault, R. H.; Okamura, K.; Su, C. J. *Macromolecules* **1970**, *3*, 735.
(18) Delsarte, J.; Weill, G. *Macromolecules* **1974**, *7*, 450.
(19) Iwakura, Y.; Iwata, K.; Matsuo, S.; Tohara, A. *Makromol. Chem.* **1969**, *122*, 275.
(20) Akita, S.; Einaga, Y.; Miyaki, Y.; Fujita, H. *Macromolecules* **1976**, *9*, 774.
(21) Tinoco, I., Jr. *J. Chem. Phys.* **1960**, *33*, 1332.
(22) Fan, C. F.; Hsu, S. L. *Macromolecules* **1991**, *24*, 6244.
(23) Fan, C. F.; Hsu, S. L. *Macromolecules* **1992**, *25*, 266.

MA945048+